Inorg. Chem. **1987**, *26*, 3473–3478 **3473**

Contribution from the Department of Chemistry and Laboratory for Molecular Structure and Bonding,
Texas A&M University, College Station, Texas 77843

Structural and Theoretical Considerations in Tantalum and Niobium $M_2Cl_6(SMe_2)_4$ and $M_2Cl_6(dto)_2$ Complexes

Jo Ann M. Canich and F. Albert Cotton*

Received June 10, 1987

The tantalum and niobium face-sharing dimers $M_2Cl_6(SMe_2)_3$ (I) have been found to react with SMe_2 to form edge-sharing bioctahedra $M_2Cl_6(SMe_2)_4$ (II). The metal–metal bond lengths of the d^2–d^2 dimers increase by ca. 0.14 Å in going from I to II, which raises a question as to the exact nature of the metal–metal bond in II [Ta–Ta = 2.829 (1) Å; $Nb–Nb_{av}$ = 2.836 [2] Å]. Compounds of the type $M_2Cl_6(dto)_2$ (III) (dto = 3,6-dithiaoctane) should be structurally similar to II and therefore were characterized by X-ray diffraction. The tantalum complex of III was found to have an average metal–metal bond length of 2.847 [6] Å while that of the niobium analogue was surprisingly shorter, 2.688 (2) Å, closely resembling the metal–metal bond length of I and those of other previously characterized edge-sharing bioctahedra of niobium and tantalum. The following crystallographic parameters were found for the four compounds: for $Ta_2Cl_6(SMe_2)_4$, space group $P2_1/n$ with a = 10.324 (5) Å, b = 11.110 (2) Å, c = 10.446 (3) Å, β = 97.07 (3)°, and Z = 2; for $Nb_2Cl_6(SMe_2)_4$, space group $P\bar{1}$ with a = 13.320 (2) Å, b = 14.159 (2) Å, c = 12.351 (3) Å, α = 91.81 (2)°, β = 92.06 (2)°, γ = 92.66 (2)°, and Z = 4; for $Ta_2Cl_6(dto)_2$, space group $P\bar{1}$ with a = 10.448 (2) Å, b = 12.424 (2) Å, c = 9.613 (2) Å, α = 92.25 (1)°, β = 101.67 (1)°, γ = 85.65 (1)°, and Z = 2; for $Nb_2Cl_6(dto)_2$, space group $Pbca$ with a = 14.639 (2) Å, b = 15.746 (2) Å, c = 10.996 (3) Å, and Z = 4. Fenske–Hall molecular orbital calculations have been utilized in the interpretation of structural data.

Introduction

Ligand substitution reactions of niobium and tantalum $M_2Cl_6(SMe_2)_3$ and $M_2Cl_6(tht)_3$ (tht = tetrahydrothiophene) complexes have been much explored, yet few of these dimeric species synthesized have been structurally characterized and those that have been contain, predominantly, phosphine ligands.[1] One type of dimeric species prepared by these reactions contains two metal atoms that are held in proximity within a set of 10 ligand atoms defining an edge-sharing bioctahedron. Complexes of this type provide the opportunity to study metal–metal interactions through a variety of ligand sets and other pertinent factors.[2]

The use of nonbridging sulfur ligands in edge-sharing bioctahedra has presented some interesting questions with regard to metal–metal bonding. For example, α-$Mo_2(\mu\text{-}SEt)_2Cl_4(dto)_2$ (dto = 3,6-dithiaoctane) contains an unusually short Mo_2^{6+} metal–metal bond distance of 2.682 (1) Å.[3] Calculations based on structural data show the energy levels of the δ and δ^* orbitals to be so close that the order of filling the orbitals remains uncertain. On the other hand, $Mo_2Cl_6(dto)_2$, which contains chelating sulfur ligands in axial/equatorial positions, has a rather long metal–metal bond distance of 2.735 (2) Å.[4] This is odd in light of the smaller bridging atom, Cl versus S. Similarly, two compounds containing terminal SMe_2 ligands, $M_2(\mu\text{-}SPh)_2Cl_6(SMe_2)_2$ (M = Ta, W), contain unusually long metal–metal bond distances, 3.165 (1) and 2.759 (1) Å, respectively.[5] Other edge-sharing bioctahedra containing terminal sulfur ligands appear entirely "normal". In continuing our study of the edge-sharing bioctahedra, we would like to report the structural characterization and theoretical calculations of two new compounds, $Ta_2Cl_6(SMe_2)_4$ (**1**) and $Nb_2Cl_6(SMe_2)_4$ (**2**), in addition to those for $Ta_2Cl_6(dto)_2$ (**3**) and $Nb_2Cl_6(dto)_2$ (**4**).[1a]

Experimental Section

Standard Schlenk and vacuum line techniques were used in the preparation of all compounds because of the air sensitivity of both products and reactants. Products were prepared, filtered, and washed under an inert atmosphere of argon. Solvents, toluene and hexane, were freshly distilled from sodium benzophenone ketyl prior to use, and were transferred to and from reaction vessels via stainless-steel cannulae and/or syringes. The compounds $Ta_2Cl_6(SMe_2)_3$ and $Nb_2Cl_6(SMe_2)_3$ were prepared by the literature method involving the sodium amalgam reduction of $TaCl_5$ or $NbCl_5$ in the presence of excess dimethyl sulfide.[6] Both $Ta_2Cl_6(dto)_2$ and $Nb_2Cl_6(dto)_2$ were prepared by a method similar to the literature preparation.[1a] Exact details are given below. Dimethyl sulfide was purchased from Aldrich Chemical Co., and 3,6-dithiaoctane (dto) was purchased from Fairfield Chemical Co. Both reagents were deaerated prior to use. Magnetic susceptibility measurements were obtained at room temperature on a MSB1 Johnson Matthey magnetic susceptibility balance. Samples were loaded in a nitrogen atmosphere drybox and sealed with septa.

Preparation and Crystallization of $Ta_2Cl_6(SMe_2)_4$ (1). In a 100-mL round-bottom Schlenk flask, 0.015 g (0.20 mmol) of $Ta_2Cl_6(SMe_2)_3$ was dissolved in 10 mL of toluene and 1 mL (13.6 mmol) of SMe_2. The solution was filtered into a Schlenk tube, which was then layered with 0.015 mL (0.17 mmol) of MeSSMe in 10 mL of hexane. Slow diffusion of the reaction layers produced both crystalline and powdered materials. Products include the starting material, $Ta_2Cl_6(SMe_2)_3$, and small amounts of the red crystalline product $Ta_2Cl_6(SMe_2)_4$. Due to restricted quantities of the latter material, characterization was limited to X-ray diffraction. $Ta_2Cl_6(SMe_2)_4$ is formed in small quantities in similar reactions when SMe_2 is either used as a reactant or produced as a product.

Preparation and Crystallization of $Nb_2Cl_6(SMe_2)_4$ (2). In a 100-mL round-bottom Schlenk flask, 0.12 g (0.21 mmol) of $Nb_2Cl_6(SMe_2)_3$ was dissolved in 10 mL of toluene and 1 mL (13.6 mmol) of SMe_2. The solution was filtered into a Schlenk tube, which was then layered with 0.015 mL (0.17 mmol) of MeSSMe in 10 mL of hexane. Slow diffusion of the reaction layers produced a mixture of powdered and crystalline material. A large portion of the solid was identified as the starting material, $Nb_2Cl_6(SMe_2)_3$, by a unit cell determination. A small quantity of green crystalline material was also formed, and this was identified as $Nb_2Cl_6(SMe_2)_4$ by X-ray diffraction. It should be noted that this product, like $Ta_2Cl_6(SMe_2)_4$, is formed in other similar reactions involving $Nb_2Cl_6(SMe_2)_3$.

Preparation of $Ta_2Cl_6(dto)_2$ (3). The compound $Ta_2Cl_6(dto)_2$ was prepared by using a modification of the literature procedure.[1a] A toluene solution (30 mL) containing 0.75 g (0.99 mmol) of $Ta_2Cl_6(SMe_2)_3$ was filtered into a 100-mL round-bottom Schlenk flask. To this were added 0.48 mL (3.1 mmol) of dto and 10 mL of toluene. After being stirred for 1 day, the mixture produced a green oily material. The solvent was

---

(1) (a) Clay, M. E.; Brown, T. M. *Inorg. Chim. Acta* **1983**, *72*, 75. Cotton, F. A.; Roth, W. J. *Inorg. Chim. Acta* **1983**, *71*, 175. (c) Cotton, F. A.; Roth, W. J. *Inorg. Chem.* **1983**, *22*, 3654. (d) Cotton, F. A.; Falvello, L. R.; Najjar, R. S. *Inorg. Chem.* **1983**, *22*, 375. (e) Cotton, F. A.; Duraj, S. A.; Falvello, L. R.; Roth, W. J. *Inorg. Chem.* **1985**, *24*, 4389. (f) Chakravarty, A. R.; Cotton, F. A.; Diebold, M. P.; Lewis, D. B.; Roth, W. J. *J. Am. Chem. Soc.* **1986**, *108*, 971. (g) Clay, M. E.; Brown, T. M. *Inorg. Chim. Acta* **1982**, *58*, 1. (h) Allen, A. D.; Naito, S. *Can. J. Chem.* **1976**, *54*, 2948. (i) Cotton, F. A.; Diebold, M. P.; Roth, W. J. *Inorg. Chem.* **1985**, *24*, 3507.

(2) Cotton, F. A. *Polyhedron* **1987**, *6*, 667.

(3) Cotton, F. A.; Diebold, M. P.; O'Connor, C. J.; Powell, G. L. *J. Am. Chem. Soc.* **1985**, *107*, 7438.

(4) Cotton, F. A.; Fanwick, P. E.; Fitch, J. W. *Inorg. Chem.* **1978**, *17*, 3254.

(5) (a) Campbell, G. C.; Canich, J. M.; Cotton, F. A.; Duraj, S. A.; Haw, J. F.; *Inorg. Chem.* **1986**, *25*, 287. (b) Boorman, P. M.; Ball, J. M.; Moynihan, K. J.; Patel, V. D.; Richardson, J. F. *Can. J. Chem.*, **1984**, *61*, 3809.

(6) Cotton, F. A.; Najjar, R. C. *Inorg. Chem.* **1981**, *20*, 2716. The procedure for bulk preparation of $Ta_2Cl_6(SMe_2)_3$ and $Nb_2Cl_6(SMe_2)_3$ has been adapted from: Templeton, J. L.; McCarley, R. E. *Inorg. Chem.* **1978**, *17*, 2293.

0020-1669/87/1326-3473$01.50/0

decanted, and the oil was washed several times with 10-mL aliquots of hexane and/or toluene, until a light green powder was obtained. The product, $Ta_2Cl_6(dto)_2$, was obtained in 54% yield. $\chi_M = -1.09 \times 10^{-4}$ cgsu.

Crystallization of $Ta_2Cl_6(dto)_2$ (3). X-ray crystallographic quality crystals were grown by filtering 0.15 g (0.20 mmol) of $Ta_2Cl_6(SMe_2)_3$ in toluene solution (30 mL) into a Schlenk tube, which was then layered with a 0.1 mL of (0.65 mmol) of dto in hexane solution (15 mL). Diffusion between layers caused growth of amber-green crystals.

Preparation of $Nb_2Cl_6(dto)_2$ (4). The compound $Nb_2Cl_6(dto)_2$ was prepared by using a modified literature preparation.[1a] A toluene solution (20 mL) of $Nb_2Cl_6(SMe_2)_3$ (0.65 g, 1.1 mmol) was filtered into a 100-mL round-bottom Schlenk flask. To this was added 0.54 mL (3.5 mmol) of dto in 15 mL of toluene. After 1 day of stirring, a dark purple solid was generated. The solvent was decanted off, and the solid was washed with two 10-mL aliquots of hexane. The product, $Nb_2Cl_6(dto)_2$, was pumped to dryness and was recovered in a 52% yield. $\chi_M = -2.88 \times 10^{-4}$ cgsu.

Crystallization of $Nb_2Cl_6(dto)_2$ (4). X-ray crystallographic quality crystals were generated by dissolving 0.12 g (0.21 mmol) of $Nb_2Cl_6(SMe_2)_3$ in 15 mL of toluene, which was then filtered into a Schlenk tube, and layered with 0.1 mL (0.65 mmol) of 3,6-dithiaoctane in hexane solution (15 mL). From this, a mixture of deep red crystals (~95%) and amber-green crystals (~5%) was formed. The two types of crystals have been identified as structural isomers of $Nb_2Cl_6(dto)_2$.

Crystallographic Study. Crystals of compounds 1–4 were grown as described above. All crystals were mounted in glass capillary tubes with epoxy resin in order to protect these air-sensitive substances.

The geometric and intensity data of compounds 1–4 were gathered with one of three automated four-circle diffractometers equipped with Mo Kα radiation. Routine unit cell identification and intensity data collection procedures have been fully described elsewhere.[7] To ascertain crystal quality and to verify lattice symmetry and dimensions, axial photographs were taken for all crystals. Three check reflections were used to monitor the change in intensity but showed no significant variation. Empirical absorption corrections based on azimuthal scans of χ near 90° were applied to all data sets. Corrections were made for Lorentz and polarization effects. Standard computational procedures were used to solve and refine structures with the VAX-SDP software package on a VAX-11/780 computer.

Structure Solution and Refinement of $Ta_2Cl_6(SMe_2)_4$ (1). The possibility of an orthorhombic *c*-centered cell was dismissed after a photograph was taken of the alleged *c*-diagonal. Data collection was therefore based on the monoclinic primitive cell. From systematic absences, the space group $P2_1/n$ was uniquely determined. The Patterson map was used to determine the coordinates for the tantalum atom. The remaining nonhydrogen atoms were located by a series of alternating difference Fourier maps and least squares refinements. Final residuals were 0.044 88 (R) and 0.059 08 (R_w). Three peaks in the final difference Fourier map of approximately 1.4 e/Å^3 remained due to series termination errors.

Structure Solution and Refinement of $Nb_2Cl_6(SMe_2)_4$ (2). The centrosymmetric space group $P\bar{1}$ was chosen for the triclinic cell and found to be correct on the basis of a successful refinement. Of the four unique niobium atoms, one was located from the Patterson map. The other three were obtained from a difference Fourier map after refinement of the first niobium atom. The metal atoms are related by inversion centers in such a way that the unit cell contains four independent dimers (four half-dimers per asymmetric unit). A series of alternating difference Fourier maps and least squares refinements led to the location of the remaining non-hydrogen atoms for all four half-dimers. Prior to final anisotropic refinement, an additional empirical absorption correction was made.[8] Final residuals were calculated at 0.054 07 (R) and 0.075 75 (R_w). One peak over 1.0 e/Å^3 was observed in the final difference Fourier map and was attributed to a series termination error.

Structure Solution and Refinement of $Ta_2Cl_6(dto)_2$ (3). The compound crystallizes in the space group $P\bar{1}$. The first independent tantalum atom was located by use of a Patterson map. After least-squares refinement of this atom, the second unique tantalum atom was located in a difference Fourier map. The independent tantalum atoms are positioned about inversion centers so that the asymmetric unit contains two half-dimers for a total of two dimers per unit cell. By employment of a series of least-squares refinements and difference Fourier maps, the remaining non-hydrogen atoms for both half-dimers were located. All atoms were refined anisotropically to give residuals of 0.038 63 (R) and 0.052 71 (R_w). Three peaks over 1.0 e/Å^3 in the final difference Fourier map were accounted for by a series termination error.

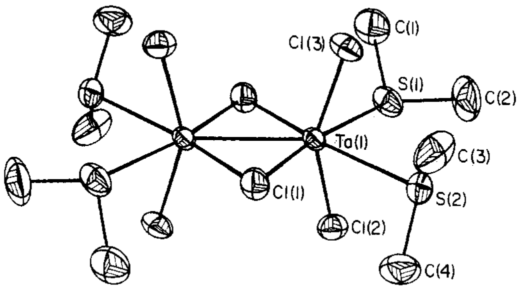

Figure 1. Structure and labeling scheme for $Ta_2Cl_6(SMe_2)_4$. Atoms are represented by their 50% probability ellipsoids.

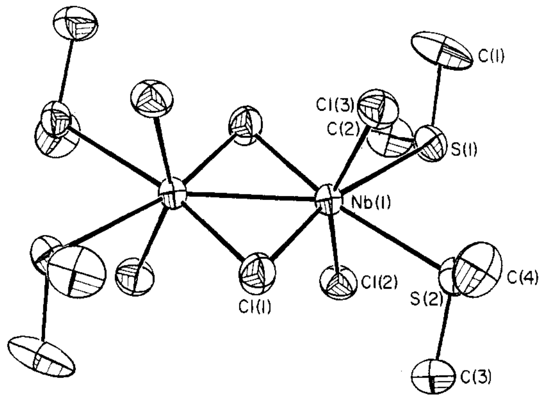

Figure 2. Structure and labeling scheme for $Nb_2Cl_6(SMe_2)_4$. Atoms are represented by their 50% probability ellipsoids.

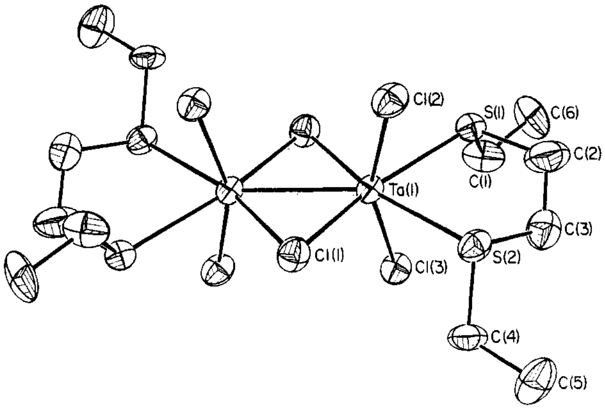

Figure 3. Structure and labeling scheme for $Ta_2Cl_6(dto)_2$. Atoms are represented by their 50% probability ellipsoids.

Structure Solution and Refinement of $Nb_2Cl_6(dto)_2$ (4). The compound $Nb_2Cl_6(dto)_2$ crystallizes in two different forms. The minor product produced poor quality green crystals having a unit cell (10.4798 Å, 12.4931 Å, 9.5995 Å, 92.57°, 101.74°, 84.55°) of dimensions similar to that for $Ta_2Cl_6(dto)_2$. The major form produced purple orthorhombic crystals of the space group *Pbca*. The unique niobium atom was located via the Patterson map. All other non-hydrogen atoms were found through an alternating series of least-squares refinements and difference Fourier maps. Final residuals were calculated at 0.042 45 (R) and 0.056 93 (R_w).

Additional crystallographic parameters for the data collection and structure refinement are given in Table I. Fractional atomic coordinates for compounds 1 through 4 are found in Tables II–V, and selected bond distances and angles are given in Table VI. ORTEP views of 1–4 are shown in Figures 1–4, respectively.

Results and Discussion

Syntheses. The compounds $Ta_2Cl_6(SMe_2)_4$ (1) and $Nb_2Cl_6(SMe_2)_4$ (2) were obtained as unexpected side products in the attempted oxidative-addition reaction of dimethyl disulfide with either $Ta_2Cl_6(SMe_2)_3$ or $Nb_2Cl_6(SMe_2)_3$, in the presence of di-

---

(7) See, for example: Bino, A.; Cotton, F. A.; Fanwick, P. E. *Inorg. Chem.* **1979**, *18*, 3558.

(8) Walker, W.; Stuart, D. *Acta Crystallogr., Sect. A: Cryst. Phys., Diffr., Theor. Gen. Crystallogr.* **1983**, *A39*, 158.

Table I. Crystal Data for $Ta_2Cl_6(SMe_2)_4$ (**1**), $Nb_2Cl_6(SMe_2)_4$ (**2**), $Ta_2Cl_6(dto)_2$ (**3**), and $Nb_2Cl_6(dto)_2$ (**4**)

	1	**2**	**3**	**4**
formula	$Ta_2Cl_6S_4C_8H_{24}$	$Nb_2Cl_6S_4C_8H_{24}$	$Ta_2Cl_6S_4C_{12}H_{28}$	$Nb_2Cl_6S_4C_{12}H_{28}$
fw	823.15	647.07	875.21	699.14
space group	$P2_1/n$	$P\bar{1}$	$P\bar{1}$	Pbca
syst abs	$h0l$ ($h + l \neq 2n$) $0k0$ ($k \neq 2n$)			$h0l$ ($l \neq 2n$) $0kl$ ($k \neq 2n$) $hk0$ ($h \neq 2n$)
a, Å	10.324 (5)	13.320 (2)	10.448 (2)	14.639 (2)
b, Å	11.110 (2)	14.159 (2)	12.424 (2)	15.746 (2)
c, Å	10.446 (3)	12.351 (3)	9.613 (2)	10.996 (3)
α, deg		91.81 (2)	92.25 (1)	
β, deg	97.07 (3)	92.06 (2)	101.67 (1)	
γ, deg		92.66 (2)	85.65 (1)	
V, Å	1189 (1)	2324 (1)	1218 (1)	2535 (1)
Z	2	4	2	4
d_{calcd}, g/cm^3	2.299	1.849	2.386	1.832
cryst size, mm	0.7 × 0.5 × 0.1	0.4 × 0.3 × 0.2	0.1 × 0.3 × 0.4	0.3 × 0.3 × 0.4
μ(Mo Kα), cm^{-1}	106.81	19.787	104.346	18.213
data collcn instrum	CAD-4	Syntex P3	Syntex P3	Syntex $P\bar{1}$
radiation (monochromated in incident beam)	Mo Kα (λ_α = 0.710 73 Å)			
orientation reflcns: no.; range (2θ), deg	25; 16.2–36.3	25; 20.0–29.9	25; 20.6–29.5	15; 20.4–29.4
temp, °C	22	22	25	4
scan method	ω–2θ	ω–2θ	ω–2θ	ω–2θ
data collcn range (2θ), deg	4–50	4–45	4–45	4–45
no. of unique data; tot. no. with $F_o^2 > 3\sigma(F_o^2)$	2081; 1758	6114; 4373	3205; 2307	1995; 1069
no. of params refined	91	361	217	109
transmissn factors: max; min	0.9967; 0.6093	0.9992; 0.9321	0.9996; 0.8091	0.9982; 0.9081
R^a	0.044 88	0.054 07	0.038 63	0.042 45
$R_w{}^b$	0.059 08	0.075 75	0.052 71	0.056 93
quality-of-fit indicator^c	1.9343	1.597	1.120	1.099
largest shift/esd, final cycle	0.00	0.05	0.00	0.00
largest peak, e/Å^3	1.465	2.967	1.298	0.533

[a] $R = \sum||F_o| - |F_c||/\sum|F_o|$. [b] $R_w = [\sum w(|F_o| - |F_c|)^2/\sum w|F_o|^2]^{1/2}$; $w = 1/\sigma(|F_o|^2)$. [c] Quality of fit $= [\sum w(|F_o| - |F_c|)^2/(N_{observns} - N_{params})]^{1/2}$.

Table II. Atomic Positional Parameters and Equivalent Isotropic Displacement Parameters and Their Estimated Standard Deviations for $Ta_2Cl_6(SMe_2)_4$

atom	x	y	z	B,^{a} Å^2
Ta(1)	0.10944 (3)	0.07696 (4)	0.00278 (3)	2.107 (8)
Cl(1)	0.0474 (3)	−0.0360 (3)	0.1736 (2)	3.32 (5)
Cl(2)	0.0275 (3)	0.2657 (3)	0.0613 (3)	3.29 (5)
Cl(3)	0.2757 (3)	−0.0512 (3)	−0.0517 (3)	3.48 (5)
S(1)	0.1992 (3)	0.2252 (3)	−0.1710 (3)	3.76 (6)
S(2)	0.3066 (3)	0.1612 (3)	0.1781 (3)	3.29 (5)
C(1)	0.219 (1)	0.138 (2)	−0.313 (1)	5.5 (3)
C(2)	0.366 (1)	0.273 (1)	−0.121 (2)	6.5 (4)
C(3)	0.413 (1)	0.040 (1)	0.235 (2)	6.0 (3)
C(4)	0.234 (1)	0.196 (1)	0.321 (1)	5.1 (3)

[a] B values for anisotropically refined atoms are given in the form of the isotropic equivalent thermal parameter defined as $^4/_3[a^2\beta_{11} + b^2\beta_{22} + c^2\beta_{33} + ab(\cos\gamma)\beta_{12} + ac(\cos\beta)\beta_{13} + bc(\cos\alpha)\beta_{23}]$. Estimated standard deviations in the least significant digits are given in parentheses.

methyl sulfide. These same side products, **1** and **2**, have also been identified in several other oxidative-addition reactions involving disulfides, even when dimethyl sulfide was not added. We believe that the additional equivalent of dimethyl sulfide needed in the formation of **1** and **2** according to eq 2 is produced as a product of the oxidative-addition reaction, eq 1.

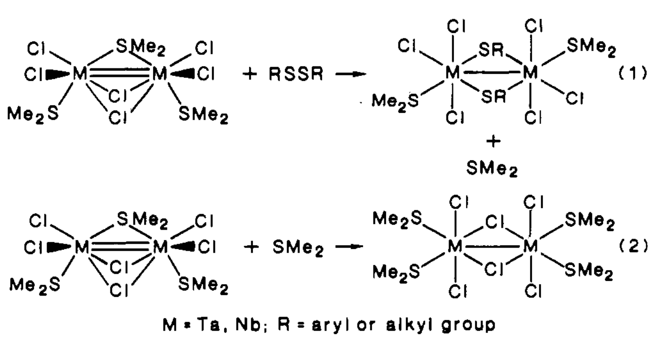

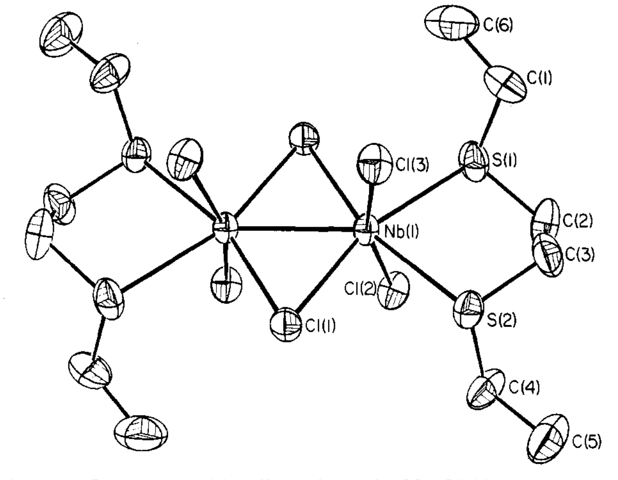

Figure 4. Structure and labeling scheme for $Nb_2Cl_6(dto)_2$. Atoms are represented by their 50% probability ellipsoids.

Interestingly, the starting materials $Ta_2Cl_6(SMe_2)_3$ and $Nb_2Cl_6(SMe_2)_3$ are routinely prepared in the presence of excess dimethyl sulfide, yet $Ta_2Cl_6(SMe_2)_4$ and $Nb_2Cl_6(SMe_2)_4$ have not been identified in these reaction mixtures. This may be due to the workup employed, which involves extraction of the $M_2Cl_6(SMe_2)_3$ compounds by toluene or benzene from insoluble reaction components that might well include compounds **1** and **2** as minor reaction products. Evidently, the equilibrium existing between the two species strongly favors the face-sharing bioctahedron over the edge-sharing bioctahedron. This is indicated by the high reaction yields of $Ta_2Cl_6(SMe_2)_3$ and $Nb_2Cl_6(SMe_2)_3$ even in the presence of excess dimethyl sulfide and by the fact that an independent treatment of these materials with dimethyl sulfide gave evidence only for $M_2Cl_6(SMe_2)_3$ in the reaction mixture. Traces of $M_2Cl_6(SMe_2)_4$ may have been present, but the amounts were too small to permit detection or characterization. Our chance isolation of these $M_2Cl_6(SMe_2)_4$ species evidently depends on the fortuitous existence of appropriate conditions for their separation

Table III. Atomic Positional Parameters and Equivalent Isotropic Displacement Parameters and Their Estimated Standard Deviations for $Nb_2Cl_6(SMe_2)_4$

atom	*x*	*y*	*z*	*B*,[a] Å^2
Nb(1)	0.08473 (8)	0.03621 (7)	0.06360 (8)	2.49 (2)
Cl(1)	0.0611 (2)	-0.1150 (2)	-0.0165 (3)	4.00 (7)
Cl(2)	0.1904 (2)	0.1032 (2)	-0.0672 (2)	3.70 (6)
Cl(3)	0.0415 (3)	-0.0000 (2)	0.2423 (2)	4.04 (7)
S(1)	0.1602 (3)	0.2019 (2)	0.1681 (3)	3.99 (7)
S(2)	0.2688 (2)	-0.0159 (2)	0.1399 (2)	3.44 (6)
C(1)	0.082 (1)	0.227 (1)	0.283 (1)	7.1 (4)
C(2)	0.127 (1)	0.2974 (9)	0.084 (1)	5.1 (3)
C(3)	0.334 (1)	-0.070 (1)	0.029 (1)	5.7 (3)
C(4)	0.255 (1)	-0.1173 (9)	0.225 (1)	5.4 (3)
Nb(1a)	0.57417 (8)	0.95282 (7)	0.44202 (8)	2.86 (2)
Cl(1a)	0.5799 (3)	1.1110 (2)	0.5014 (3)	4.36 (7)
Cl(2a)	0.5294 (3)	0.9771 (2)	0.2575 (3)	4.50 (7)
Cl(3a)	0.6773 (3)	0.8934 (2)	0.5806 (2)	4.25 (7)
S(1a)	0.5728 (4)	0.7725 (3)	0.3498 (3)	6.3 (1)
S(2a)	0.7612 (3)	0.9893 (2)	0.3618 (3)	3.99 (7)
C(1a)	0.617 (2)	0.691 (1)	0.445 (1)	6.9 (5)
C(2a)	0.658 (2)	0.762 (1)	0.245 (1)	8.3 (5)
C(3a)	0.845 (1)	1.041 (1)	0.472 (1)	4.9 (3)
C(4a)	0.756 (1)	1.090 (1)	0.276 (1)	6.0 (4)
Nb(1b)	0.56147 (8)	0.43433 (7)	0.05128 (9)	3.10 (2)
Cl(1b)	0.6132 (3)	0.5760 (2)	-0.0273 (3)	4.64 (7)
Cl(2b)	0.5685 (3)	0.4878 (3)	0.2354 (3)	5.27 (8)
Cl(3b)	0.6017 (3)	0.3309 (2)	-0.0920 (3)	5.57 (8)
S(1b)	0.5451 (3)	0.2599 (2)	0.1420 (3)	4.58 (8)
S(2b)	0.7636 (3)	0.4368 (4)	0.1056 (4)	7.6 (1)
C(1b)	0.482 (2)	0.269 (1)	0.270 (1)	9.1 (5)
C(2b)	0.447 (1)	0.189 (1)	0.069 (2)	6.5 (4)
C(3b)	0.796 (1)	0.340 (1)	0.180 (2)	11.5 (5)
C(4b)	0.835 (1)	0.420 (2)	-0.013 (2)	11.2 (7)
Nb(1c)	1.05564 (8)	0.56400 (7)	0.43659 (8)	3.01 (2)
Cl(1c)	1.1154 (2)	0.4361 (2)	0.5300 (3)	4.99 (8)
Cl(2c)	1.1109 (3)	0.6865 (3)	0.5609 (3)	5.79 (9)
Cl(3c)	1.0421 (3)	0.4927 (3)	0.2603 (3)	5.57 (9)
S(1c)	1.0285 (4)	0.7232 (3)	0.3223 (4)	7.1 (1)
S(2c)	1.2457 (4)	0.5964 (4)	0.3655 (5)	8.9 (1)
C(1c)	0.941 (2)	0.693 (2)	0.204 (1)	14.7 (7)
C(2c)	0.944 (1)	0.7959 (9)	0.394 (1)	6.3 (4)
C(3c)	1.317 (2)	0.609 (2)	0.475 (2)	19.7 (8)
C(4c)	1.292 (1)	0.487 (1)	0.310 (2)	8.5 (5)

[a] See footnote *a* in Table II.

from solution in crystalline form. We do not know how to reproduce these conditions in any other deliberate way.

The formation of $Ta_2Cl_6(dto)_2$ (**3**) and $Nb_2Cl_6(dto)_2$ (**4**) followed a preparative route similar to that reported in the literature.[1a] The major differences involve the starting material, $M_2Cl_6(SMe_2)_3$ versus $M_2Cl_6(tht)_3$ (tht = tetrahydrothiophene), and the stoichiometry of dto used in the reaction, which was much larger in the literature preparation. The reaction can probably be regarded as a ligand displacement reaction, where the first step involves substitution of the terminal dimethyl sulfide ligands by dangling dto ligands, eq 3. While this particular reaction intermediate was never isolated, the participation of such a species is indicated in similar ligand displacement reactions, where compounds containing dangling ligands such as $Nb_2Cl_6(SMe_2)(MeSCH_2SMe)_2$[9] and $Ta_2Cl_6(SMe_2)(dppm)_2$[10] have been structurally characterized.

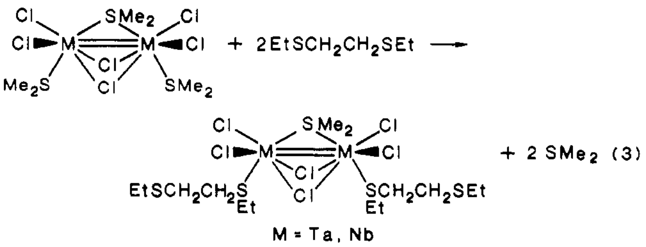

Table IV. Atomic Positional Parameters and Equivalent Isotropic Displacement Parameters and Their Estimated Standard Deviations for $Ta_2Cl_6(dto)_2$

atom	*x*	*y*	*z*	*B*,[a] Å^2
Ta(1)	0.12561 (6)	0.03313 (5)	0.06586 (6)	2.30 (1)
Cl(1)	-0.0202 (4)	-0.0538 (3)	0.1735 (4)	3.36 (9)
Cl(2)	0.2637 (5)	-0.1218 (3)	0.0322 (5)	3.6 (1)
Cl(3)	0.0705 (4)	0.2114 (3)	0.1402 (4)	3.11 (9)
S(1)	0.3318 (4)	0.1163 (3)	-0.0009 (4)	2.78 (8)
S(2)	0.2897 (4)	0.0310 (3)	0.3160 (4)	3.11 (9)
C(1)	0.302 (2)	0.261 (1)	-0.032 (2)	4.2 (4)
C(2)	0.455 (2)	0.114 (2)	0.165 (2)	5.8 (6)
C(3)	0.397 (2)	0.139 (2)	0.294 (2)	4.5 (5)
C(4)	0.210 (2)	0.089 (2)	0.450 (2)	3.7 (4)
C(5)	0.301 (2)	0.103 (2)	0.598 (2)	5.2 (5)
C(6)	0.417 (2)	0.303 (1)	-0.084 (2)	5.1 (5)
Ta(1a)	0.36860 (6)	0.53522 (5)	0.43744 (6)	2.22 (1)
Cl(1a)	0.5225 (4)	0.4385 (4)	0.3243 (4)	3.37 (9)
Cl(2a)	0.2507 (5)	0.3872 (3)	0.4788 (5)	3.68 (9)
Cl(3a)	0.3969 (4)	0.7102 (3)	0.3665 (4)	3.15 (9)
S(1a)	0.1426 (4)	0.6281 (3)	0.4985 (4)	3.03 (9)
S(2a)	0.2077 (4)	0.5225 (3)	0.1868 (4)	2.81 (9)
C(1a)	0.131 (2)	0.774 (1)	0.509 (2)	4.0 (4)
C(2a)	0.025 (2)	0.606 (2)	0.332 (2)	4.1 (4)
C(3a)	0.080 (2)	0.629 (2)	0.199 (2)	3.7 (4)
C(4a)	0.284 (2)	0.578 (1)	0.053 (2)	3.6 (4)
C(5a)	0.200 (2)	0.566 (2)	-0.096 (2)	3.9 (4)
C(6a)	0.214 (2)	0.811 (2)	0.650 (2)	5.2 (5)

[a] See footnote *a* in Table II.

Table V. Atomic Positional Parameters and Equivalent Isotropic Displacement Parameters and Their Estimated Standard Deviations for $Nb_2Cl_6(dto)_2$

atom	*x*	*y*	*z*	*B*,[a] Å^2
Nb(1)	0.04716 (6)	0.01144 (6)	0.10357 (8)	2.26 (2)
Cl(1)	-0.0789 (2)	-0.0891 (2)	0.0838 (2)	2.93 (5)
Cl(2)	-0.1605 (2)	0.0965 (2)	-0.0715 (3)	3.43 (6)
Cl(3)	-0.0433 (2)	0.1219 (2)	0.1934 (3)	3.37 (6)
S(1)	0.1952 (2)	0.0898 (2)	0.1772 (3)	3.75 (7)
S(2)	0.0436 (2)	-0.0409 (2)	0.3322 (3)	3.16 (6)
C(1)	0.176 (1)	0.1990 (8)	0.235 (1)	5.4 (4)
C(2)	0.2200 (8)	0.0322 (9)	0.318 (1)	4.8 (3)
C(3)	0.1316 (9)	0.0236 (8)	0.398 (1)	4.4 (3)
C(4)	0.0912 (9)	-0.1488 (8)	0.348 (1)	4.5 (3)
C(5)	0.087 (1)	-0.1774 (9)	0.483 (1)	5.9 (4)
C(6)	0.159 (1)	0.2597 (9)	0.127 (1)	6.4 (4)

[a] See footnote *a* in Table II.

Rearrangement of this intermediate species with concomitant loss of dimethyl sulfide would produce compounds **3** and **4**, eq 4.

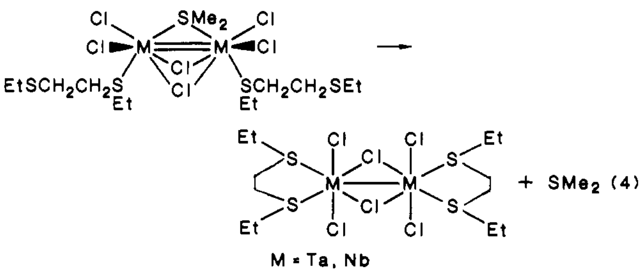

The possibility of different isomers with regard to conformations of the chelating sulfur ligands exists. Experimentally, only two forms were found, one for $Ta_2Cl_6(dto)_2$ (green) and two for $Nb_2Cl_6(dto)_2$ (purple and green) with the green minor component, approximately 5% of the reaction mixture, being of the same form as that for the tantalum species. This will be discussed in greater detail with the structural results. In the original preparation of $Nb_2Cl_6(dto)_2$, two isomers were postulated based on the complexity of the infrared spectrum when compared to that for the tantalum species.[1a]

Structures. Compounds **1**–**4** contain M_2^{6+} cores of niobium or tantalum. The atoms M(1), Cl(1), S(1), and S(2) and their symmetry-related counterparts are roughly coplanar with Cl(3)

---

(9) Canich, J. M.; Cotton, F. A., unpublished results.

(10) Cotton, F. A.; Krichbaum, G.; Meadows, J. H., unpublished results.

Table VI. Selected Bond Distances (Å) and Angles (deg) for $Ta_2Cl_6(SMe_2)_4$ (**1**), $Nb_2Cl_6(SMe_2)_4$ (**2**, **2a**, **2b**, **2c**), $Ta_2Cl_6(dto)_2$ (**3**, **3a**), and $Nb_2Cl_6(dto)_2$ (**4**)

	1	**3**	**3a**	**4**		**1**	**3**	**3a**	**4**
M(1)–M(1)′	2.829 (1)	2.841 (1)	2.852 (1)	2.688 (2)	M(1)–Cl(3)	2.353 (2)	2.365 (4)	2.361 (4)	2.399 (3)
M(1)–Cl(1)	2.334 (2)	2.352 (4)	2.351 (4)	2.440 (3)	M(1)–S(1)	2.698 (2)	2.659 (4)	2.710 (4)	2.622 (3)
M(1)–Cl(1)′	2.343 (2)	2.356 (4)	2.364 (4)	2.440 (3)	M(1)–S(2)	2.730 (2)	2.656 (4)	2.651 (4)	2.647 (3)
M(1)–Cl(2)	2.370 (2)	2.368 (4)	2.379 (4)	2.401 (3)					

	2	**2a**	**2b**	**2c**		**2**	**2a**	**2b**	**2c**
M(1)–M(1)′	2.836 (2)	2.840 (2)	2.833 (2)	2.834 (2)	M(1)–Cl(3)	2.366 (2)	2.357 (3)	2.354 (3)	2.369 (3)
M(1)–Cl(1)	2.333 (3)	2.331 (3)	2.342 (3)	2.333 (3)	M(1)–S(1)	2.771 (3)	2.762 (3)	2.747 (3)	2.728 (3)
M(1)–Cl(1)′	2.348 (2)	2.343 (3)	2.332 (3)	2.330 (3)	M(1)–S(2)	2.736 (2)	2.747 (3)	2.750 (4)	2.733 (4)
M(1)–Cl(2)	2.373 (2)	2.375 (3)	2.371 (3)	2.354 (3)					

	1	**3**	**3a**	**4**		**1**	**3**	**3a**	**4**
M(1)′–M(1)–Cl(1)	52.93 (5)	52.9 (1)	53.0 (1)	56.59 (7)	Cl(1)′–M(1)–Cl(2)	98.10 (7)	97.4 (2)	96.5 (2)	95.7 (1)
M(1)′–M(1)–Cl(1)′	52.65 (5)	52.8 (1)	52.6 (1)	56.58 (7)	Cl(1)′–M(1)–Cl(3)	98.42 (8)	95.7 (1)	95.0 (1)	95.1 (1)
M(1)′–M(1)–Cl(2)	103.34 (5)	102.1 (1)	102.1 (1)	97.79 (8)	Cl(1)′–M(1)–S(1)	81.43 (7)	87.4 (1)	90.7 (1)	82.41 (9)
M(1)′–M(1)–Cl(3)	103.54 (6)	100.8 (1)	101.1 (1)	99.36 (8)	Cl(1)′–M(1)–S(2)	168.54 (7)	166.5 (1)	169.3 (1)	164.2 (1)
M(1)′–M(1)–S(1)	134.01 (5)	140.06 (9)	143.04 (9)	138.54 (9)	Cl(2)–M(1)–Cl(3)	153.13 (7)	157.1 (2)	156.6 (2)	162.8 (1)
M(1)′–M(1)–S(2)	138.47 (5)	140.6 (1)	138.1 (1)	138.87 (8)	Cl(2)–M(1)–S(1)	78.27 (7)	77.0 (1)	75.6 (1)	78.9 (1)
Cl(1)–M(1)–Cl(1)′	105.58 (6)	105.8 (1)	105.6 (1)	113.17 (7)	Cl(2)–M(1)–S(2)	77.52 (7)	80.1 (1)	80.7 (1)	86.14 (9)
Cl(1)–M(1)–Cl(2)	97.93 (8)	97.1 (2)	98.0 (2)	92.88 (9)	Cl(3)–M(1)–S(1)	83.41 (7)	85.0 (1)	84.0 (1)	89.3 (1)
Cl(1)–M(1)–Cl(3)	97.86 (8)	97.2 (2)	98.4 (2)	95.14 (9)	Cl(3)–M(1)–S(2)	82.17 (7)	82.8 (1)	84.2 (1)	79.9 (1)
Cl(1)–M(1)–S(1)	172.54 (7)	166.3 (1)	163.2 (1)	163.2 (1)	S(1)–M(1)–S(2)	87.29 (7)	79.2 (1)	78.6 (1)	82.5 (1)
Cl(1)–M(1)–S(2)	85.60 (7)	87.7 (1)	85.1 (1)	82.39 (9)	M(1)–Cl(1)–M(1)′	74.42 (6)	74.2 (1)	74.4 (1)	66.83 (7)

	2	**2a**	**2b**	**2c**		**2**	**2a**	**2b**	**2c**
M(1)′–M(1)–Cl(1)	52.96 (6)	52.77 (7)	52.54 (7)	52.52 (7)	Cl(1)′–M(1)–Cl(2)	97.6 (1)	99.3 (1)	97.4 (1)	98.1 (1)
M(1)′–M(1)–Cl(1)′	52.46 (7)	52.39 (7)	52.86 (7)	52.62 (7)	Cl(1)′–M(1)–Cl(3)	97.2 (1)	97.6 (1)	98.7 (1)	97.9 (1)
M(1)′–M(1)–Cl(2)	102.90 (7)	103.80 (8)	103.28 (8)	103.9 (1)	Cl(1)′–M(1)–S(1)	88.39 (8)	78.9 (1)	86.91 (9)	87.0 (1)
M(1)′–M(1)–Cl(3)	103.18 (8)	103.23 (8)	103.44 (9)	103.59 (9)	Cl(1)′–M(1)–S(2)	166.77 (9)	167.97 (9)	172.5 (1)	166.8 (1)
M(1)′–M(1)–S(1)	140.79 (7)	131.09 (9)	139.66 (8)	139.55 (9)	Cl(2)–M(1)–Cl(3)	153.9 (1)	153.0 (1)	153.3 (1)	152.5 (1)
M(1)′–M(1)–S(2)	140.73 (7)	139.58 (7)	132.9 (1)	140.5 (1)	Cl(2)–M(1)–S(1)	77.41 (9)	77.1 (1)	82.6 (1)	76.9 (1)
Cl(1)–M(1)–Cl(1)′	105.42 (7)	105.16 (8)	105.40 (8)	105.14 (8)	Cl(2)–M(1)–S(2)	79.39 (9)	79.80 (9)	77.0 (1)	81.0 (1)
Cl(1)–M(1)–Cl(2)	98.0 (1)	97.4 (1)	98.6 (1)	98.7 (1)	Cl(3)–M(1)–S(1)	81.61 (9)	85.6 (1)	77.1 (1)	81.6 (1)
Cl(1)–M(1)–Cl(3)	98.7 (1)	98.4 (1)	97.5 (1)	98.6 (1)	Cl(3)–M(1)–S(2)	81.31 (9)	79.34 (9)	84.9 (1)	78.3 (2)
Cl(1)–M(1)–S(1)	165.98 (9)	173.8 (1)	167.3 (1)	167.7 (1)	S(1)–M(1)–S(2)	78.38 (8)	89.2 (1)	87.5 (1)	79.9 (1)
Cl(1)–M(1)–S(2)	87.78 (8)	86.82 (9)	80.5 (1)	88.0 (1)	M(1)–Cl(1)–M(1)′	74.58 (7)	74.84 (8)	74.60 (8)	74.86 (8)

and Cl(2) located above and below the plane to form a distorted edge-sharing bioctahedron. The molecules, which are illustrated in Figures 1–4, all reside on positions of crystallographic inversion symmetry, located at the midpoint of the metal–metal vector. The compounds $Ta_2Cl_6(dto)_2$ (**3**) and $Nb_2Cl_6(SMe_2)_4$ (**2**) contain two and four independent dimers per unit cell, respectively. Bond distances and bond angles vary only slightly from one molecule to the next. Subsequent values given in the text are averages of these, and numbers in brackets are calculated values for the variance. Figures 2 and 3 portray only one representative molecule for each compound.

For compounds **1**–**3**, deviation from octahedral geometry about the metal centers is especially severe. This is seen in the Cl(3)–M–Cl(2) bond angle, which for an octahedron would be at 180°, that averages 153° for compounds **1** and **2** and is slightly greater for compound **3** at 157°. The crystallographically characterized isomer of $Nb_2Cl_6(dto)_2$, compound **4**, has the smallest deviation from linearity of the Cl(3)–M–Cl(2) bond angle at 163°. Evidence for metal–metal interaction is seen in all four compounds by the wider than 90° Cl(1)–M–Cl(1)′ bond angle of approximately 105° for compounds **1**–**3**, and at 113° for compound **4**. Corresponding to this is a relatively short metal–metal bond distance for compound **4**, measured at 2.688 (2) Å, which is, in fact, shorter than the metal–metal distance of any other Nb(III) or Ta(III) edge-sharing bioctahedral compound containing chlorine bridges. Typical values range from 2.692 (2) Å for β-$Ta_2Cl_6(dmpm)_2$[1e] to 2.729 (2) Å for $Nb_2Cl_6(dppe)_2$.[1b] In sharp contrast to this are the extremely long metal–metal bond distances for compounds **1**–**3**: 2.847 [6] Å for $Ta_2Cl_6(dto)_2$, 2.829 (1) Å for $Ta_2Cl_6(SMe_2)_4$, and 2.836 [2] Å for $Nb_2Cl_6(SMe_2)_4$. These distances more closely approximate values for Nb_2^{8+} core species, e.g., 2.868 (2) Å for $Nb_2Cl_4(\mu\text{-}S)_2(tht)_4$[11] and 2.866 (2) Å for $Nb_2Cl_4(\mu\text{-}S)_2(NCMe)_4$.[12] Although these latter two distances are longer by ca. 0.03 Å, it must be noted that the formal charge of the metal atoms is +4 rather than +3 and should therefore favor a longer distance. Likewise, the larger bridging atom, S versus Cl, would also tend to favor elongation of the metal–metal bond vector.

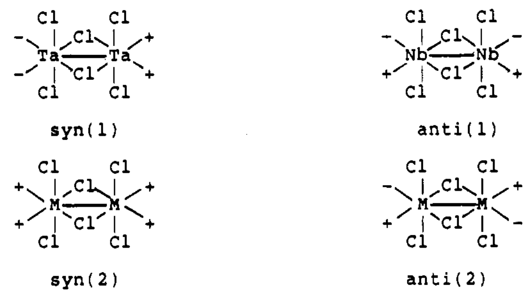

syn(1) anti(1)

syn(2) anti(2)

Figure 5. Representation of the four possible isomers of α-$M_2Cl_6(dto)_2$. Plus and minus signs indicate the up or down direction of the lone pair orbitals on the sulfur atoms.

A closer comparison of compounds **3** and **4** reveals two major structural differences in addition to the 0.16-Å difference in metal–metal bond distance. The first of these is the distinct arrangement of the sulfur ligands about the metal center in compounds **3** and **4**. Each chelate ring may have its *S*-ethyl groups syn or anti. Even with the restriction that both rings in a given molecule will be syn or anti, four isomers may exist, and these are shown in Figure 5, where the plus and minus signs represent the directions of the *S*-ethyl groups. Only two of these four geometries are possible if the molecule is required to have an inversion center, namely the anti(1) and syn(1) forms. Compound **3**, $Ta_2Cl_6(dto)_2$, has been observed only in the latter form while compound **4**, $Nb_2Cl_6(dto)_2$, has been detected in both forms with

---

[11] Drew, M. G. B.; Rice, D. A.; Williams, D. M. *J. Chem. Soc., Dalton Trans.* **1985**, 417.

[12] Benton, A. J.; Drew, M. G. B.; Hobson, R. J.; Rice, D. A. *J. Chem. Soc., Dalton Trans.* **1981**, 1304.

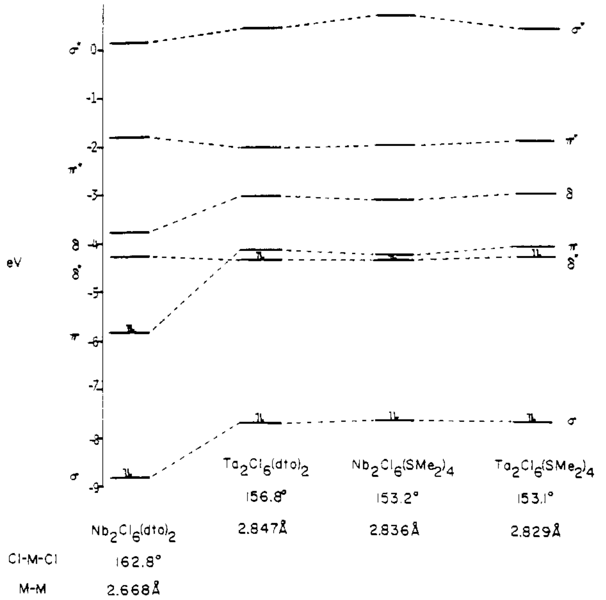

Figure 6. Diagram showing the energy levels of those MO's primarily involved in metal–metal bonding.

the major species being the anti(1) form. Only small amounts of the syn(1) form are produced in the reaction. While this form has not been structurally characterized, it possesses a unit cell nearly identical with that of $Ta_2Cl_6(dto)_2$ and can therefore be assumed to be isostructural. Related to this is the difference in M–S and M–Cl bond lengths between the two compounds. $Nb_2Cl_6(dto)_2$ has the shorter M–S bond length by ca. 0.03 Å and the longer $M{-}Cl_{br}$ and $M{-}Cl_t$ bond lengths by ca. 0.08 and 0.03 Å, respectively. The geometric arrangement of the dto ligands in $Nb_2Cl_6(dto)_2$ appears to increase the σ-donating ability of the ligand to the metal. This is reflected not only in the shorter metal–metal bond length but also in the longer M–Cl bond distances.

The second major difference between **3** and **4** involves the Cl(3)–M–Cl(2) bond angle versus metal–metal bond distance for the two species. Previously, the deviation of the Cl(3)–M–Cl(2) bond angle from linearity has been associated with steric repulsions between axial ligands.[13] If this were the determining factor in the Cl(3)–M–Cl(2) bond angle, one would predict a smaller Cl(3)–M–Cl(2) bond angle for compound **4**, which has the shorter metal–metal bond distance, and a wider Cl(3)–M–Cl(2) bond angle for the longer metal–metal-bonded tantalum complex. This is exactly opposite to what is observed experimentally! Compound **3**, with the longer metal–metal bond distance of 2.847 [6] Å, also has the more acute Cl(3)–M–Cl(2) bond angle of 156.9 [3]° while compound **4**, with the shorter metal–metal bond distance of 2.688 (2) Å, has a more obtuse Cl(3)–M–(2) bond angle of 162.8 (1)°.

Fenske–Hall Calculations. In an attempt to rationalize these latter findings, Fenske–Hall calculations were carried out on the model compound $Nb_2Cl_6(SH_2)_4$ using crystallographic coordinates for all atoms with the exception of the hydrogen atoms, which were placed at appropriate S–H bond distances along the S–C vectors observed in compounds **1**–**4**.[14] The results of the calculation are summarized in Figure 6, where only those orbitals involved in metal–metal bonding are depicted. For $Nb_2Cl_6(dto)_2$ (**4**), with the relatively short metal–metal bond distance, the expected molecular orbital energy level ordering of $\sigma \ll \pi < \delta^* < \delta < \pi^* \ll \sigma^*$ is observed indicating, unambiguously, a metal–metal double bond for the compound. For the longer metal–metal-bonded species; **1**–**3**, the π and δ* orbitals have very similar energies.

The results of the Fenske–Hall calculations are thus consistent with the structural observations on which they are based. They clearly indicate that both σ and π bonding are stronger in **4** than in the other three cases. They clearly indicate that **4** should be diamagnetic with a $\sigma^2\pi^2$ double bond, as in numerous similar Nb or Ta compounds of the type $M_2Cl_6(diphos)_2$, which have M–M bond lengths around 2.70 Å. A measurement confirmed the predicted diamagnetism.

The computational results are ambiguous concerning the ground states of compounds **1**–**3**. They do imply weaker M–M bonding, but of course, that is mainly a consequence of the longer M–M distances employed as input. They leave open the possibility that the compounds might be paramagnetic, but a measurement on **3** at room temperature showed that this is not the case. Because of the very small amounts of **1** and **2** available the magnetic susceptibilities of these could not be measured with our balance.

Concluding Remarks. The existence of significantly different Nb–Nb and Ta–Ta bond lengths in a series of four compounds having grossly similar compositions and structures has been discovered, but the reasons remain obscure. It is perhaps best to focus on the contrast between **3** and **4**, since **1** and **2** contain somewhat different ligands and also show different M–S bond lengths. In comparing **3** and **4**, we are not unmindful of the fact that they contain different metal atoms, but we consider that the comparison is nevertheless valid for two reasons. (1) In other edge-sharing bioctahedral systems that we have studied, strictly homologous Nb and Ta compounds have displayed M–M distances that were within 0.02 Å or less of each other, whereas the present difference is ca. 0.15 Å. (2) We have shown that there is an isomer of the niobium compound **4** that is crystallographically isomorphous with the tantalum compound **3**, although we were not able to obtain crystallographic quality crystals. This (niobium) isomer of **4** must certainly have a structure essentially identical with that of **3**.

The only *qualitative* difference between **3** and **4** is in the conformations of the chelate rings formed by the dto ligands, yet they show a number of quantitative differences, of which the most significant is the difference of ca. 0.15 Å in the M–M distances. While a great many factors having to do with metal–ligand interactions, especially M–S interactions, have been examined as possible causes of this, we have been unable to identify any obvious causal relationship. A subtle but important problem is that even when a reciprocity can be perceived between the change in M–M distance and a small change in some other parameter, it is not possible to say which of these should be considered to be the cause of the other.

In the final analysis, however, the observation that even conformational changes in chelate rings can give rise to a sizable change in M–M bond length is empirically valid and important. It is yet another relatively subtle factor that must be controlled in any comparative studies intended to derive information about M–M bonding from structural data.

Acknowledgment. We thank the Robert A. Welch Foundation for financial support under Grant No. A-494.

Supplementary Material Available: For the crystal structures of $Ta_2Cl_6(SMe_2)_4$, $Nb_2Cl_6(SMe_2)_4$, $Ta_2Cl_6(dto)_2$, and $Nb_2Cl_6(dto)_2$, full listings of bond distances, bond angles, and anisotropic displacement parameters (12 pages); listings of observed and calculated structure factors (51 pages). Ordering information is given on any current masthead page.

---

(13) Shaik, S.; Hoffman, R.; Fisel, C. R.; Summerville, R. H. *J. Am. Chem. Soc.* **1980**, *102*, 4555.

(14) Fenske, R. F.; Hall, M. B. *Inorg. Chem.* **1972**, *11*, 768.